

# Joint Radio Resource Allocation, 3D Placement and User Association of Aerial Base Stations in IoT Networks

Arman Azizi, Nader Mokari, Mohamad Reza Javan

**Abstract**—In this paper, a novel method for joint radio resource allocation (RRA), three-dimensional placement (3DP), and user association of aerial base stations (ABSs) as a main problem in the internet of things (IoT) networks is proposed. In our proposed model, we consider two schemes: a) line of sight (LoS) b) generalized. In the LoS scheme, all the ABSs should see the IoT users as LoS. In the generalized scheme, ABSs can see some of the IoT users as LoS and some of them as NLoS. The main goal of this paper is to minimize the overall transmit power of the IoT users while satisfying some quality of service (QoS) constraints in uplink scenario. To solve the optimization problems and to convert the main problems with high complexity into the subproblems with lower complexity, we decompose them into two subproblems namely 3DP subproblem and joint RRA and user association (JRU) subproblem. The methods which we use to solve our proposed optimization problems are Semi Definite Relaxation (SDR) and Geometric Programming (GP). Finally, using simulations, we evaluate the performance of the proposed schemes for different values of the network parameters.

**Index Terms**— Aerial Base Station, IoT, Radio Resource Allocation, 3D deployment, User Association, Geometric Programming, Semi Definite Relaxation.

## I. INTRODUCTION

### A. State of the Art

1) *Necessity to use UAVs*: The use of unmanned aerial vehicles (UAVs) in wireless communication networks has received remarkable attentions recently [1]–[5], [11]–[36]. The use of UAVs can be useful in some regions which have no cellular infrastructures or the areas in which building a cellular infrastructure is very expensive. The use of UAVs as aerial base stations (ABSs) in wireless communication networks makes lots of advantages. ABSs can be deployed in higher altitudes compared to the terrestrial base stations. Therefore, they can see ground users with higher chance of line of sight (LoS) links. More over, ABSs can easily move to updated places, and therefore, they can be more flexible than terrestrial base stations in the scenarios where users are mobile [2]. The technical challenges in ABS communication networks can be classified into optimal placement, air to ground (A2G) channel modeling, resource management, energy efficiency, and performance analysis [2]–[4]. In the next generation of wireless communications, networks will require extra dense base stations deployments not only in 2-D area but also in 3-D space. Therefore, ABSs can play an important role for wireless cellular networks in overloaded cases. Furthermore, ABSs are more robust against environmental changes [4].

2) *Necessity to use UAVs in IoT*: IoT can change the ways of wireless communications with all of the devices. An IoT system uses intelligent interfaces for connecting IoT devices to each other at anytime and anywhere which use any network and any service [5]–[8]. More over, UAVs are easy to deploy, capable of reprogramming during run time, capable of measuring anything anywhere and capable of having high mobility, therefore, they can be chosen to provide many applications, such as service delivery, farming, pollution mitigation, and rescue operations [5], [9], [10]. According to the above definitions, UAVs are the efficient option to choose for IoT network, and hence, they can play an important role. Furthermore, at the same time, they can provide extra services when they are equipped with some special devices (e.g., cameras, actuators and sensors) [5], [9], [10]. In the other hand, the transmit power of IoT devices are low in comparison with other traditional networks, and hence, IoT devices can not be able to communicate in long range. More over, ABSs can update their locations due to the new locations of IoT devices. Therefore, ABSs can collect IoT data from the IoT devices and transmit it to other devices which are out of transmission range. Accordingly, ABSs can play an important role in IoT networks which have battery-limited devices [11]–[13].

### B. Related Works

The Related works to this paper can be classified into the following items:

1) *Placement*: The authors in [14] maximize the number of users which covered by a single ABS by finding the efficient 3D placement for the ABS. In [15], the authors obtain the optimal altitude deployment of a UAV in order to maximize the coverage. In [16], the authors enhance the coverage performance in public safety communications by obtaining the optimal deployment of UAVs. In [17], the authors use the sigmoid function LoS model to optimize the UAV height in different performance metrics. In [18], the authors design the ABS enabled heterogeneous networks (HetNets) by 3D placements of ABSs as one of the important factors. In [19], the optimal altitude of a single UAV is found to achieve a required coverage with minimum transmit power. In [20], the authors find the optimal coverage range and hovering altitude of UAVs to minimize the transmit power of them. In [21], the authors propose the next generation heterogeneous network including cooperative UAVs. Accordingly, they find the optimal placement and optimal distribution of UAVs to

optimize the overall network delays. In [22], the authors study on a model which uses density and cost functions to compute the areas with higher demands, and hence, the UAVs are deployed based on these cost functions. In [23], the locations of ABSs are optimized in order to maximize the network throughput over a given geographical area. In [24], the authors maximize the fifth percentile capacity of the network by optimizing the locations of the UAVs.

2) *Power Allocation*: In [25], the authors investigate a secure wireless network based on physical layer security technique considering UAV as a relay. In order to maximize the secrecy rate, they optimize the transmit power of the source and the UAV as a relay while satisfying a sequence of information-causality constraints. These constraints ensure that the relay cannot forward the undecoded data.

3) *Joint Power Allocation and Spectrum Allocation*: In [26], the authors present a scenario including cluster heads-UAVs communications in M2M networks. They propose an efficient scheduling and resource allocation mechanism in order to minimize the transmit power of cluster heads while satisfying rate requirements of M2M devices. In [27], the authors investigate a cellular network with multi-layer UAVs. In order to minimize the packet transmission delay, the resources allocation mechanism proposed.

4) *Joint Placement and User Association*: In [28], the authors study the optimal deployment of UAVs and association of static ground users to UAVs in order to meet the users rate requirements. The work in [29] investigates a communication network based on multiple UAVs in downlink transmissions considering UAV efficient deployment and user association. In [30], the authors study on the UAV networks using the sigmoid LoS model in order to characterize the received signal strength. Accordingly, they propose the multi-objective optimization. Furthermore, the UAVs locations are found as a part of an optimization problem or they are assumed to be known. In [31], the authors present a more comprehensive placement and user association problem of a single UAV-BS. In [32], the authors present an IoT network based on UAVs. They study on deploying the UAVs efficiently in order to minimize the power consumption of the ground IoT devices by considering the required bit error rate. Furthermore, they present the efficient association of the ground IoT devices to UAVs. In [33], the authors maximize the users' quality of experience (QoE) while minimizing the transmit power of the UAVs.

5) *Joint Placement and Spectrum Allocation*: In [34], the authors propose a multi-hop D2D network based on UAV in order to develop the coverage of network. They show that deploying the UAV in an efficient way increases the data rate assuming the transmit power or distance is beyond the threshold.

6) *Adaptive Modulation*: In [35], the authors investigate a scenario in which UAVs can be used as relays between ground devices and a ground base station. They propose a method in order to control the heading angle of UAVs considering space-time coding and adaptive modulation, and hence, they optimize the performance of the ground-to-relay links. In [36], the authors maximize the energy efficiency in the network

in which ground nodes are capable of adaptive modulation. Furthermore, they show how mobility pattern of UAVs can affect on adaptive modulation.

### C. Our Contribution

The main contribution of this paper is to develop a novel approach for intelligently deploying multiple ABSs while minimizing the overall ABS transmit power needed to satisfy the users data rate in uplink scenario. Furthermore, subcarrier allocation and adaptive modulation are used in this scenario. Our contribution of this paper can be listed as follows:

- **Joint RRA, 3DP, and User Association**: The main factor of ABSs which makes them useful is the ability to move, and hence, the location of ABSs is not fixed. Therefore, we should see what is the impact of finding the location of ABSs on RRA and user association. Accordingly, it is necessary to find the radio variables, placement variables, and user association variables in a joint method. To the best of our knowledge, there is no work which consider the joint RRA, 3DP, and user association.
- **Comparing A2G channel models**: To the best of our knowledge, there is no work which provide the comparison between two A2G channel models namely only the LoS scheme and the generalized scheme. Finally, we know which one is better for our IoT Scenario.
- **Multi ABS, multi IoT users, multi subcarrier system, and adaptive modulation**: To the best of our knowledge, there is no work which has all the above items together. In this paper, we show the impact of different modulation orders on overall transmit power of IoT users. Furthermore, we show the impact of ABS numbers on the overall transmit power of the IoT users and the average ABS altitude.
- **Converting the non-convex problems into convex with relaxation methods**: We propose two main problems for our scenario which both of them are non-convex and intractable, and hence, we convert them into convex problems with semidefinite relaxation (SDR) and geometric programming (GP).
- **Computational Complexity**: We obtain the computational complexity of our proposed schemes.

## II. SYSTEM MODEL

Consider an IoT system consisting of a set  $\mathcal{I} = \{1, \dots, I\}$  including  $I$  IoT users deployed within a geographical area. In this system, a set  $\mathcal{J} = \{1, \dots, J\}$  including  $J$  ABSs should be deployed to collect the data from the ground devices in the uplink. Furthermore, a set  $\mathcal{M} = \{1, \dots, M\}$  including  $M$  modulation orders should be assigned to each user for uplink transmission. The  $m^{th}$  modulation order shows that we use  $2^{m+1}$ PSK for transmission. The locations of user  $i$  and ABS  $j$  are, respectively, given by  $(\hat{x}_i; \hat{y}_i)$  and  $(x_j; y_j; h_j)$ . We assume that devices transmit in the uplink using orthogonal frequency division multiple access (OFDMA). Note that, we consider a network in which the locations of devices are known to a control center such as a central cloud server. The ground IoT devices can be mobile (e.g., smart cars) and their data availability can be intermittent (e.g., sensors). For A2G

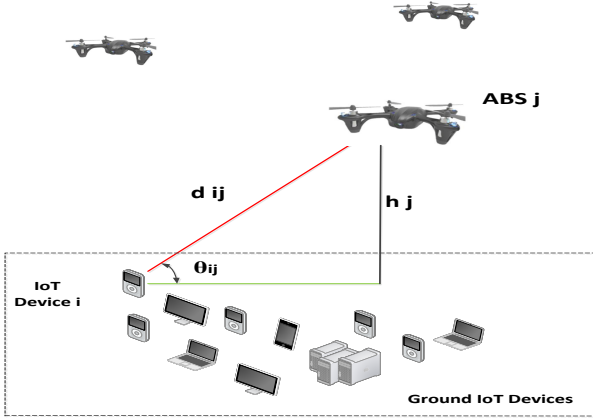


Fig. 1. System Model

communications, each device can typically have a LoS view towards a specific ABS with a given probability. This LoS probability depends on the environment, location of the device and the ABS, and the elevation angle between the device and the ABS [4]. One suitable expression for the LoS probability between ABS  $j$  and user  $i$  is given by [4]:

$$Pr_{LoS,ij} = \frac{1}{1 + \alpha \exp(-\beta(\frac{180}{\pi}\theta_{ij} - \alpha))}, \quad \forall i, j, \quad (1)$$

where  $\alpha$  and  $\beta$  are constant values which depend on the carrier frequency and type of environment such as rural, urban, or dense urban, and  $\theta_{ij}$  is the elevation angle that is defined as follows:

$$\theta_{ij} = \frac{180}{\pi} \times \sin^{-1}\left(\frac{h_j}{d_{ij}}\right), \quad \forall i, j, \quad (2)$$

and  $d_{ij}$  is the distance between device  $i$  and ABS  $j$  given by

$$d_{ij} = \sqrt{(x_j - \hat{x}_i)^2 + (y_j - \hat{y}_i)^2 + h_j^2}, \quad \forall i, j. \quad (3)$$

The path loss expressions for LoS and NLoS connections are as follows [4]:

$$L_{LoS,ij} = 10n \log\left(\frac{4\pi f_c d_{ij}}{c}\right) + \xi_{LoS}, \quad \forall i, j, \quad (4)$$

$$L_{NLoS,ij} = 10n \log\left(\frac{4\pi f_c d_{ij}}{c}\right) + \xi_{NLoS}, \quad \forall i, j, \quad (5)$$

where  $n$  is the path loss exponent,  $L_{LoS,ij}$  and  $L_{NLoS,ij}$  are the average path loss for LoS and NLoS links, respectively.  $\xi_{LoS}$  and  $\xi_{NLoS}$  are the average additional loss in addition to the free space propagation loss which depend on the environment,  $c$  is the speed of light, and  $f_c$  is the carrier frequency. Finally, the average path loss as a function of the ABS altitude and coverage radius can be written as [15]:

$$\bar{L}(x_j, y_j, h_j) = Pr_{LoS,ij} L_{LoS,ij} + Pr_{NLoS,ij} L_{NLoS,ij}, \quad (6)$$

TABLE I  
SIMULATION PARAMETERS

$i$	IoT user indicator
$j$	ABS indicator
$m$	Modulation order indicator
$l$	Subcarrier indicator
$(\hat{x}_i; \hat{y}_i)$	2D location of the $i^{th}$ user
$(x_j; y_j; h_j)$	3D location of the $j^{th}$ ABS
$\alpha$	Constant value depends on environment
$\beta$	Constant value depends on environment
$\theta_{ij}$	Elevation angle of ABS
$Pr_{LoS,ij}$	LoS probability between ABS $j$ and user $i$
$d_{ij}$	Distance between device $i$ and ABS $j$
$n$	Path loss exponent
$L_{LoS,ij}$	Average path loss for LoS link
$L_{NLoS,ij}$	Average path loss for NLoS link
$\xi_{LoS}$	Average additional loss of LoS link
$\xi_{NLoS}$	Average additional loss of NLoS link
$c$	Speed of light
$f_c$	Carrier frequency
$\bar{L}(x_j, y_j, h_j)$	Average Path loss
$Pr_{NLoS,ij}$	NLoS probability between ABS $j$ and user $i$
$P_{imj}^{receive}$	Received power from the $j^{th}$ ABS
$\hat{r}_{ij}$	Symbol rate of the $j^{th}$ UAV to the $i^{th}$ user
$P_{imj}^{transmit}$	Transmit power of IoT user
$r_{imj}$	Transmission bit rate
$N_0$	Noise power spectral density
$\epsilon$	Threshold for LoS probability
$\rho_{imj}^l$	Binary variable for RRA and user association
$\tau_i$	Threshold of transmission rate for each user
$\delta$	Bit error rate requirement

where  $Pr_{NLoS,ij}$  is NLoS probability between ABS  $j$  and user  $i$ . Therefore, we obtain a closed-form for average path loss by substituting (1), (4), and (5) into (6) as follows:

$$\bar{L}(x_j, y_j, h_j) = 10n \log\left(\frac{4\pi f_c d_{ij}}{c}\right) + Pr_{LoS,ij}(\xi_{LoS} - \xi_{NLoS}) + \xi_{NLoS}. \quad (7)$$

For minimum phase shift keying (MPSK) modulation, the bit error rate expression is given by [37]:

$$BER_{imj} = \frac{2}{m+1} Q\left(\sqrt{\frac{2P_{imj}^{receive}}{\hat{r}_{ij} N_0}} \sin\left(\frac{\pi}{2^{m+1}}\right)\right), \quad (8)$$

where  $P_{imj}^{receive}$  is the received power from the  $j^{th}$  ABS to the  $i^{th}$  user when using the  $m^{th}$  modulation order for transmission,  $\hat{r}_{ij}$  is the symbol rate of the  $i^{th}$  user to the  $j^{th}$  ABS,  $N_0$  is the noise power spectral density and  $Q(\cdot)$  is the Q-function. In the next step, we propose the closed-form formulation for transmit power of the following schemes.

#### A. The Case with only the LoS

By using (4), (8),  $P_{imj}^{transmit} = P_{imj}^{receive} \times 10^{\frac{L_{LoS,ij}}{10}}$ , and considering  $n = 2$ , the minimum transmit power of ABS  $j$  needed to reach a bit error rate requirement of  $\delta$  is given by

$$P_{imj}^{transmit} = A_m \cdot r_{imj} \cdot d_{ij}^2, \quad (9)$$

where  $P_{imj}^{transmit}$  is the transmit power and  $r_{imj} = \hat{r}_{ij}(m+1)$  is the transmission bit rate from the the  $i^{th}$  user to the  $j^{th}$  ABS by using the  $m^{th}$  modulation order for transmission,

respectively.  $A_m$  is a constant that only changes by the modulation order as follows:

$$A_m = (Q^{-1}(\frac{1}{2}\delta(m+1))) \times \frac{1}{\sin(\frac{\pi}{2^{m+1}})}^2 \times \frac{1}{(m+1)} \times \frac{1}{2} N_0 \times (\frac{4\pi f_c}{c})^2 \times 10^{\frac{\xi_{LoS}}{10}}, \quad (10)$$

where  $Q^{-1}(\cdot)$  is the inverse Q-function.

In the LoS model, the necessary condition for connecting a device to the UAV is to have a LoS probability greater than a threshold ( $\varepsilon$  is closed to 1). In other words,  $Pr_{LoS}(\theta_{ij}) \geq \varepsilon$ , and hence,  $\theta_{ij} \geq Pr_{LoS}^{-1}(\varepsilon)$  leading to:

$$d_{ij} \leq \frac{h_j}{\sin(Pr_{LoS}^{-1}(\varepsilon))}, \quad \forall i, j. \quad (11)$$

Note that (11) guarantees the user  $i$  can connect to ABS  $j$  if the distance between them is not greater than  $\frac{h_j}{\sin(Pr_{LoS}^{-1}(\varepsilon))}$ . Our goal is to maximizing the overall transmit power of the IoT users in the joint scenario including RRA, 3DP and user association. Accordingly, the objective function is given by:

$$\min_{\rho, \mathbf{x}, \mathbf{y}, \mathbf{h}} \sum_{j=1}^J \sum_{m=1}^M \sum_{i=1}^I \sum_{l=1}^L P_{imj}^{\text{transmit}} \rho_{imj}^l, \quad (12)$$

where  $\rho_{imj}^l$  is a binary variable that is one if there is a connection between the  $i^{\text{th}}$  user and the  $j^{\text{th}}$  UAV using the  $m^{\text{th}}$  modulation order in the  $l^{\text{th}}$  subcarrier, and is zero otherwise. By substituting (9) into (12), our optimization problem can be formulated as:

$$\min_{\rho, \mathbf{x}, \mathbf{y}, \mathbf{h}} \sum_{j=1}^J \sum_{m=1}^M \sum_{i=1}^I \sum_{l=1}^L A_m r_{imj} d_{ij}^2 \rho_{imj}^l \quad (13a)$$

$$s.t. \quad \rho_{imj}^l \in \{0, 1\}, \quad \forall i, m, j, l, \quad (13b)$$

$$\sum_{j=1}^J \sum_{m=1}^M \sum_{l=1}^L r_{imj} \rho_{imj}^l \geq \tau_i, \quad \forall i, \quad (13c)$$

$$\rho_{imj}^l + \rho_{im'j'}^l \leq 1, \quad \forall i, j \neq j', m, l, m', l', \quad (13d)$$

$$\rho_{imj}^l + \rho_{im'j}^l \leq 1, \quad \forall i, j, l, m \neq m', \quad (13e)$$

$$\sum_{m=1}^M \sum_{i=1}^I \sum_{j=1}^J \rho_{imj}^l = 1, \quad \forall l, \quad (13f)$$

$$\rho_{imj}^l d_{ij} \leq \frac{h_j}{\sin(Pr_{LoS}^{-1}(\varepsilon))}, \quad \forall i, j, m, l. \quad (13g)$$

Constraint (13c) states that the transmission rate for each user is greater than or equal to a threshold  $\tau_i$ . Constraint (13d) guarantees that only one UAV can be assigned to each user. Constraint (13e) shows that for each ABS, each user and each subcarrier, we can use at most one modulation order. Constraint (13f) shows that the subcarriers are orthogonal in OFDMA. More over, it guarantees that for each subcarrier we have at most one modulation and one assignment of UAV to user. Constraint (13g) is the necessary condition for connecting a device to a UAV to have a LoS probability greater than a threshold.

## B. Generalized Scheme (Jonit NLoS and LoS)

In this model, by using (7), (8),  $P_{imj}^{\text{transmit}} = P_{imj}^{\text{receive}} \times 10^{\frac{L(x_j, y_j, h_j)}{10}}$ , and considering  $n = 2$ , the minimum transmit power of UAV  $j$  needed to reach a bit error rate requirement of  $\delta$  is given by:

$$P_{imj}^{\text{transmit}} = B_m \times r_{imj} \times d_{ij}^2 \times 10^{\frac{Pr_{LoS, ij}(\xi_{LoS} - \xi_{NLoS})}{10}}, \quad (14)$$

where  $B_m$  is a constant that only changes by the modulation order as follows:

$$B_m = (Q^{-1}(\frac{1}{2}\delta(m+1))) \times \frac{1}{\sin(\frac{\pi}{2^{m+1}})}^2 \times \frac{1}{(m+1)} \times \frac{1}{2} N_0 \times (\frac{4\pi f_c}{c})^2 \times 10^{\frac{\xi_{NLoS}}{10}}. \quad (15)$$

Therefore, our optimization problem in this case can be demonstrated as follows:

$$\min_{\rho, \mathbf{x}, \mathbf{y}, \mathbf{h}} \sum_{j=1}^J \sum_{m=1}^M \sum_{i=1}^I \sum_{l=1}^L B_m r_{imj} \rho_{imj}^l d_{ij}^2 \times 10^{\frac{\eta}{1+\alpha \exp(-\beta(\frac{180}{\pi} \sin^{-1}(\frac{h_j}{d_{ij}}) - \alpha))}} \quad (16a)$$

$$s.t. \quad (13b) - (13f), \quad (16b)$$

where  $\eta = \frac{(\xi_{LoS} - \xi_{NLoS})}{10}$ .

## III. SOLUTION

### A. The Case with only the Line of Sight

Our optimization problem is Mixed Integer Nonlinear Programming (MINLP), nonconvex, and NP-hard. To solve the resulting optimization problem, it is decomposed into 3DP subproblem and JRU subproblem which are iteratively solved until convergence to a local solution.

1) *3DP*: The 3DP subproblem can be formulated as Quadratically Constrained Quadratic Program (QCQP) for a fixed vector  $\rho$  as follows:

$$\min_{\mathbf{x}, \mathbf{y}, \mathbf{h}} \sum_{j=1}^J \sum_{m=1}^M \sum_{i=1}^I \sum_{l=1}^L A_m r_{imj} \rho_{imj}^l d_{ij}^2 \quad (17a)$$

$$s.t. \quad \rho_{imj}^l d_{ij} \leq \frac{h_j}{\sin(Pr_{LoS}^{-1}(\varepsilon))}, \quad \forall i, j \in \Omega, \forall m, l, \quad (17b)$$

where  $\Omega = \{(i, j) \mid \rho_{imj}^l \in \rho_0 \quad \forall m, l\}$  and  $\rho_0$  is an initial matrix for iterative method.

Note that by using (3), (17) can be transformed into (18) as follows:

$$\min_{\mathbf{x}, \mathbf{y}, \mathbf{h}} \sum_{j=1}^J \sum_{m=1}^M \sum_{i=1}^I \sum_{l=1}^L A_m r_{imj} \rho_{imj}^l ((x_j - \hat{x}_i)^2 + (y_j - \hat{y}_i)^2 + h_j^2) \quad (18a)$$

$$s.t. \quad \rho_{imj}^l (x_j - \hat{x}_i)^2 + \rho_{imj}^l (y_j - \hat{y}_i)^2 + \rho_{imj}^l h_j^2 (1 - \frac{1}{\sin^2(Pr_{LoS}^{-1}(\varepsilon))}) \leq 0. \quad (18b)$$

As we can see from (18), the optimization problem is a QCQP whose general form is given by [39], [40]:

$$\min_{\mathbf{v}} \frac{1}{2} \mathbf{v}^T \mathbf{W}_0 \mathbf{v} + \mathbf{Q}_0^T \mathbf{v} + \tilde{r}_0 \quad (19a)$$

$$s.t. \quad \frac{1}{2} \mathbf{v}^T \mathbf{W}_i \mathbf{v} + \mathbf{Q}_i^T \mathbf{v} + \tilde{r}_i \leq 0, \quad \forall i. \quad (19b)$$

Given (18), we have:

$$\mathbf{v} = [x_1 \quad y_1 \quad h_1 \quad \dots \quad x_J \quad y_J \quad h_J]_{3J \times 1}^T, \quad (20)$$

$$\mathbf{W}_0 = \begin{bmatrix} \mathbf{\Gamma}_1 & 0 & 0 & 0 \\ 0 & \cdot & 0 & 0 \\ 0 & 0 & \cdot & 0 \\ 0 & 0 & 0 & \mathbf{\Gamma}_J \end{bmatrix}_{3J \times 3J}, \quad (21)$$

where  $\mathbf{\Gamma}_j$  is a matrix which can be written as follows:

$$\mathbf{\Gamma}_j = \begin{bmatrix} 2LM\omega_j & 0 & 0 \\ 0 & 2LM\omega_j & 0 \\ 0 & 0 & 2LM\omega_j \end{bmatrix}_{3 \times 3}, \quad \forall j \in J, \quad (22)$$

and  $\omega_j = \sum_i \sum_m \sum_l A_m r_{imj} \rho_{imj}^l$ . Also we have:

$$\mathbf{W}_i = \begin{bmatrix} \Upsilon_{i1} & 0 & 0 & 0 \\ 0 & \cdot & 0 & 0 \\ 0 & 0 & \cdot & 0 \\ 0 & 0 & 0 & \Upsilon_{iJ} \end{bmatrix}_{3J \times 3J}, \quad (23)$$

where  $\Upsilon_{ij}$  is a matrix that can be written as follows:

$$\Upsilon_{ij} = \begin{bmatrix} 2LM\vartheta_{ij} & 0 & 0 \\ 0 & 2LM\vartheta_{ij} & 0 \\ 0 & 0 & 2LM\kappa\vartheta_{ij} \end{bmatrix}_{3J \times 3J}, \quad (24)$$

where  $\kappa = 1 - \frac{1}{\sin^2(\text{Pr}_{\text{LoS}}^{-1}(\epsilon))}$  and  $\vartheta_{ij} = \sum_m \sum_l A_m r_{imj} \rho_{imj}^l$ ,

Furthermore, we have:

$$\mathbf{Q}_0 = [\mathbf{\Lambda}_1 \quad \dots \quad \mathbf{\Lambda}_J]_{3J \times 1}^T, \quad (25)$$

where  $\mathbf{\Lambda}_j$  is a matrix that can be formulated as follows:

$$\mathbf{\Lambda}_j = \begin{bmatrix} -2LM \sum_i \vartheta_{ij} \hat{x}_i & -2LM \sum_i \vartheta_{ij} \hat{y}_i & 0 \end{bmatrix}_{1 \times 3},$$

$$\mathbf{Q}_i = [\Theta_{i1} \quad \dots \quad \Theta_{iJ}]_{3J \times 1}^T,$$

$$\Theta_{ij} = [-2LM\vartheta_{ij}\hat{x}_i \quad -2LM\vartheta_{ij}\hat{y}_i \quad 0]_{1 \times 3},$$

$$\tilde{r}_0 = LMJ \sum_i \gamma_i (\hat{x}_i^2 + \hat{y}_i^2),$$

$$\gamma_i = \sum_m \sum_j \sum_l A_m r_{imj} \rho_{imj}^l, \quad \text{and} \quad \tilde{r}_i = LMJ (\hat{x}_i^2 + \hat{y}_i^2) \gamma_i.$$

Note that  $\mathbf{W}_i$  is not a positive semidefinite matrix, and hence, the QCQP problem in (19) is nonconvex. Therefore, in order to solve the NP-hard problem (19), we should convert the nonconvex QCQP problem into a semidefinite programming problem by semidefinite programming relaxation (SDR) method.

First of all, we should convert the non-homogeneous QCQP problem into homogeneous QCQP problem. The homogeneous form of problem (19) can be formulated as follows [40]:

$$\min_{\mathbf{v}, a} \frac{1}{2} [\mathbf{v}^T \quad a] \begin{bmatrix} \mathbf{W}_0 & \mathbf{Q}_0 \\ \mathbf{Q}_0^T & 0 \end{bmatrix} [\mathbf{v}^T \quad a]^T + \tilde{r}_0 \quad (26a)$$

$$s.t. \quad \frac{1}{2} [\mathbf{v}^T \quad a] \begin{bmatrix} \mathbf{W}_i & \mathbf{Q}_i \\ \mathbf{Q}_i^T & 0 \end{bmatrix} [\mathbf{v}^T \quad a]^T + \tilde{r}_i, \quad (26b)$$

$$\frac{1}{2} [\mathbf{v}^T \quad a] \begin{bmatrix} 0 & 0 \\ 0 & 1 \end{bmatrix} [\mathbf{v}^T \quad a]^T + \tilde{r}_i. \quad (26c)$$

The problem (26) can be formulated as the following equivalent problem:

$$\min_{\mathbf{u}, \mathbf{U}} \frac{1}{2} \text{tr}(\mathbf{T}_0 \mathbf{U}) + \tilde{r}_0 \quad (27a)$$

$$s.t. \quad \frac{1}{2} \text{tr}(\mathbf{T}_i \mathbf{U}) + \tilde{r}_i \leq 0, \quad (27b)$$

$$\mathbf{U} = \mathbf{u}^T \mathbf{u}, \quad (27c)$$

$$\mathbf{u} \begin{bmatrix} 0 & 0 \\ 0 & 1 \end{bmatrix} \mathbf{u}^T = 1, \quad (27d)$$

where  $\mathbf{u} = [\mathbf{v}^T \quad a]_{1 \times (1+3J)}$ ,  $\mathbf{T}_0 = \begin{bmatrix} \mathbf{W}_0 & \mathbf{Q}_0 \\ \mathbf{Q}_0^T & 0 \end{bmatrix}$  and

$\mathbf{T}_i = \begin{bmatrix} \mathbf{W}_i & \mathbf{Q}_i \\ \mathbf{Q}_i^T & 0 \end{bmatrix}$ . The constraint (27c) is equivalent to  $\text{rank}(\mathbf{U}) = 1$  and  $\mathbf{U} \succeq 0$  (shows the matrix  $\mathbf{U}$  is semi definite positive (SDP)). Furthermore, the constraint (27d) is equivalent to  $a^2 = 1$ .

In the next step, we should convert the nonconvex homogeneous QCQP problem (27) into an SDP problem. The constraint  $\text{rank}(\mathbf{U}) = 1$  makes the optimization problem (27) nonconvex. Therefore, we should relax the optimization problem (27) by ignoring  $\text{rank}(\mathbf{U}) = 1$ . Finally, the convex relaxed problem can be written as follows:

$$\min_{\mathbf{U}} \frac{1}{2} \text{tr}(\mathbf{T}_0 \mathbf{U}) + \tilde{r}_0 \quad (28a)$$

$$s.t. \quad \frac{1}{2} \text{tr}(\mathbf{T}_i \mathbf{U}) + \tilde{r}_i \leq 0, \quad (28b)$$

$$\mathbf{U} \succeq 0, \quad (28c)$$

$$\text{tr}(\mathbf{H} \mathbf{U}) = 1, \quad (28d)$$

where the constraint (28d) is equivalent to  $a^2 = 1$  because  $\mathbf{H} = \begin{bmatrix} 0 & 0 \\ 0 & 1 \end{bmatrix}_{(3J+1) \times (3J+1)}$ . By solving the problem (28),

we reach to optimal  $\mathbf{U}$  denoted  $\mathbf{U}^*$ . Then, we should find  $\mathbf{u}^*$  by Gaussian Randomization Procedure (GRP) [40].

---

#### Algorithm 1 Gaussian Randomization Procedure (GRP)

---

**s1:** Choose a feasible solution  $\mathbf{U}^*$  for the relaxed homogeneous QCQP problem (28).

**s2:** For  $g = 1, \dots, G$  generate  $\mathbf{k}_g \sim \mathcal{N}(0, \mathbf{U}^*)$  with zero mean and nonzero covariance.

**s3:** Determine  $g^*$  in  $\text{argmin} \{ \mathbf{k}_g^T \mathbf{T}_0 \mathbf{k}_g + \tilde{r}_0 \}$  for the homogeneous QCQP.

**s4:** Output  $\mathbf{u}^* = \mathbf{k}_{g^*}$  for the homogeneous QCQP.

---

As we know that  $\mathbf{u} = [\mathbf{v}^T \quad a]$ , we can find  $\mathbf{v}^*$ . Therefore, the relaxed convex-3DP problem can be solved by some existing optimization tools such as CVX.

2) *Jonit RRA and User Association (JRU)*: The JRU sub-problem can be formulated as Binary Linear Programming (BLP) for fixed  $\mathbf{x}, \mathbf{y}, \mathbf{h}$  as follows:

$$\min_{\rho} \sum_{j=1}^J \sum_{m=1}^M \sum_{i=1}^I \sum_{l=1}^L A_m r_{imj} \rho_{imj}^l d_{ij}^2 \quad (29a)$$

$$s.t. \quad (13b) - (13g). \quad (29b)$$

Therefore, JRU subproblem as a Binary Linear Programming can be solved by some existing optimization tools such as NOMAD. Finally, the main problem can be solved by Algorithm 2. where  $t$  is the iteration number,  $T$  is the upper bound for

**Algorithm 2** Iterative procedure of obtaining optimal solution

**s1:** Initialize  $\rho$  from the feasible set.

**s2:** Calculate  $\mathbf{x}^*, \mathbf{y}^*, \mathbf{h}^*$  from 3DP subproblem for fixed  $\rho$ .

**s3:** Calculate obj1 and obj2 from (17a) and (29a), respectively.

**s4:** for  $t = 1$  to  $T$  do

**s4:** While  $|\text{obj1} - \text{obj2}| \geq \sigma$  or  $t < T$  calculate  $\rho^*$  from the JRU subproblem for fixed  $\mathbf{x}, \mathbf{y}, \mathbf{h}$  and  $\mathbf{x}^*, \mathbf{y}^*, \mathbf{h}^*$  from 3DP subproblem for fixed  $\rho$ .

**s4:** Set  $t = t + 1$

**s4:** end for

**s5:**  $(\rho^*, \mathbf{x}^*, \mathbf{y}^*, \mathbf{h}^*)$  is the optimal solution.

the iteration number,  $\sigma$  is a number close to zero, obj1 and obj2 are the objectives of 3D placement subproblem and joint RRA and user association subproblem, respectively.

### B. Generalized Model

Our optimization problem in the general case is also a MINP which is nonconvex and NP-hard. Therefore, to solve the problem, we decompose it into 3DP subproblem and JRU subproblem.

1) *3DP*: The 3DP subproblem can be formulated as geometric programming problem [38], [39] for a fixed  $\rho$  as follows:

$$\min_{\mathbf{x}, \mathbf{y}, \mathbf{h}} \sum_{j=1}^J \sum_{m=1}^M \sum_{i=1}^I \sum_{l=1}^L B_m r_{imj} \rho_{imj}^l d_{ij}^2 \times 10^{\frac{\eta}{1 + \alpha \exp(-\beta(\frac{180}{\pi} \sin^{-1}(\frac{h_j}{d_{ij}}) - \alpha))}} \quad (30)$$

The 3DP subproblem can be transformed into the following problem:

$$\min_{\mathbf{x}, \mathbf{y}, \mathbf{h}, \mathbf{t}_0, \mathbf{t}_1, \mathbf{f}_0} \sum_{j=1}^J \sum_{m=1}^M \sum_{i=1}^I \sum_{l=1}^L B_m r_{imj} \rho_{imj}^l (t_{0,ij}^2 + t_{1,ij}^2 + h_j^2) \times 10^{\frac{\eta}{1 + \alpha \exp(-\beta(\frac{180}{\pi} \sin^{-1}(\frac{h_j}{d_{ij}}) - \alpha))}} \quad (31a)$$

$$s.t. \quad \frac{1}{2} x_j (\hat{x}_i)^{-\frac{1}{2}} t_{0,ij}^{-\frac{1}{2}} = 1, \quad \forall i, j \in \Omega, \quad (31b)$$

$$\frac{1}{2} y_j (\hat{y}_i)^{-\frac{1}{2}} t_{1,ij}^{-\frac{1}{2}} = 1, \quad \forall i, j \in \Omega, \quad (31c)$$

$$f_{0,ij}^{-2} t_{0,ij}^2 h_j^{-2} + f_{0,ij}^{-2} t_{1,ij}^2 h_j^{-2} + f_{0,ij}^{-2} \leq 1, \quad \forall i, j \in \Omega, \quad (31d)$$

where  $d_{ij}^2$  in (30) is transformed into  $t_{0,ij}^2 + t_{1,ij}^2 + h_j^2$  in (31a) as explained before in the LoS scheme. (31d) is the posynomial form of  $\frac{d_{ij}}{h_j} \leq f_{0,ij}$ .

**Proposition 1:**  $f$  can be approximated by a monomial if and only if  $F(y) = \log f(e^y)$  can be approximated by an affine function. Furthermore,  $f$  can be approximated by a generalized posynomial if and only if  $F$  can be approximated by a convex function [38].

By Proposition 1, we can show that the function  $\sin^{-1}(\frac{1}{f_{0,ij}})$  can be approximated by a monomial if the function  $\log(\sin^{-1}(\exp(-f_{0,ij})))$  is affine. It can be shown that this function is affine for  $f_{0,ij} \geq 0.2$  and this condition always is established because  $1 \leq \frac{d_{ij}}{h_j} \leq f_{0,ij}$ . Therefore, we have  $\sin^{-1}(\frac{1}{f_{0,ij}}) \approx \mu_2 f_{0,ij}^{\omega_2}$ .

By substituting  $\sin^{-1}(\frac{1}{f_{0,ij}}) \approx \mu_2 f_{0,ij}^{\omega_2}$  into (31a) and using the following approximations [38]:

$$\exp\left(\frac{180}{\pi} \beta \mu_2 f_{0,ij}^{\omega_2}\right) \approx \left(1 + \frac{180}{\pi} \beta \mu_2 f_{0,ij}^{\omega_2}\right)^\psi, \quad (32)$$

$$10^{\eta \mu_3 f_{1,ij}^{\psi - \omega_3}} \approx \left(1 + \frac{\eta \mu_3 f_{1,ij}^{\psi - \omega_3} \log_e^{10}}{\phi}\right)^\phi, \quad (33)$$

$$f_{1,ij}^\psi + \alpha \exp(\alpha \beta) \approx \mu_3 f_{1,ij}^{\omega_3}, \quad (34)$$

where (32) and (33) are approximated for large amount of  $\psi$  and  $\phi$ , respectively, our 3DP subproblem can be demonstrated as a GP problem. Furthermore, (34) shows monomial approximation for  $f_{1,ij}^\psi + \alpha \exp(\alpha \beta)$ . Finally, the 3DP subproblem in the form of GP can be obtained as follows:

$$\min_{\mathbf{x}, \mathbf{y}, \mathbf{h}, \mathbf{t}_0, \mathbf{t}_1, \mathbf{f}_0, \mathbf{f}_1, \mathbf{f}_2} \sum_{j=1}^J \sum_{m=1}^M \sum_{i=1}^I \sum_{l=1}^L B_m r_{imj} \rho_{imj}^l (t_{0,ij}^2 + t_{1,ij}^2 + h_j^2) \times f_{2,ij}^\phi \quad (35a)$$

$$s.t. \quad (31b), (31c), (31d), \quad (35b)$$

$$f_{1,ij}^{-1} + \frac{180}{\pi} \beta \mu_2 f_{0,ij}^{\omega_2} \psi^{-1} f_{1,ij}^{-1} \leq 1, \quad \forall i, j \in \Omega, \quad (35c)$$

$$f_{2,ij}^{-1} + \frac{\eta \mu_3 f_{1,ij}^{\psi - \omega_3} \log_e^{10}}{\phi} f_{2,ij}^{-1} \leq 1, \quad \forall i, j \in \Omega, \quad (35d)$$

where (35c) and (35d) come from the exponential terms that approximated for large amount of  $\psi$  and  $\phi$  in (32) and (33), respectively. Therefore, the 3DP subproblem as a geometric programming can be solved by some existing optimization tools such as CVX.

2) *JRU*: The JRU subproblem can be formulated as Binary Linear Programming (BLP) for fixed  $\mathbf{x}, \mathbf{y}, \mathbf{h}$  as follows:

$$\min_{\rho} \sum_{j=1}^J \sum_{m=1}^M \sum_{i=1}^I \sum_{l=1}^L A_m r_{imj} \rho_{imj}^l d_{ij}^2 \times 10^{\frac{\eta}{1+\alpha \exp(-\beta(\frac{180}{\pi} \sin^{-1}(\frac{b_j}{d_{ij}}))-\alpha))} \quad (36a)$$

$$s.t. \quad (13b) - (13f), \quad (36b)$$

Therefore, the JRU subproblem as a BLP can be solved by some existing optimization tools such as NOMAD. Finally, the main problem can be solved by an iterative algorithm similar to Algorithm 2.

#### IV. COMPUTATIONAL COMPLEXITY

Here, we discuss the computational complexity of our proposed optimization problems, namely, LoS scheme and generalized scheme. Moreover, each of the proposed methods is decomposed into two subproblems namely JRU and 3DP. Therefore, we should compute the complexity of each of the subproblems in both of the proposed methods.

In the 3DP subproblem of LoS scheme, we use SDR in order to relax the 3DP subproblem, and hence, its computational complexity can be formulated as follows:

$$\max \{3J + 1, I + 1\}^3 (3J + 1)^{0.5} \log(1/\tilde{\mu}), \quad (37)$$

where  $\tilde{\mu} > 0$  is used for the given accuracy solution of interior point method (IPM). SDR is a computationally efficient approximation approach to QCQP in the sense that its complexity is polynomial in the problem size and the number of constraints. The computational complexity of JRU subproblem in the LoS scheme can be written as follows:

$$\frac{\log(\frac{4IMJL+I+L}{\tilde{t}\tilde{\mu}})}{\log(\tilde{\xi})}, \quad (38)$$

where  $\tilde{\mu}$  is used for the accuracy updating of interior point method (IPM),  $\tilde{\xi}$  is the stopping criterion for IPM, and  $\tilde{t}$  is the initial point for approximating the accuracy of IPM.

The computational complexity formulation of JRU subproblem in the generalized scheme is the same as (38). Furthermore, the computational complexity of 3DP subproblem in the generalized scheme can be written as follows:

$$\frac{\log(\frac{5IJ}{\tilde{t}\tilde{\mu}})}{\log(\tilde{\xi})}. \quad (39)$$

The computational complexity of the proposed problems can be listed in the Table II as follows:

#### V. SIMULATION RESULTS

In our simulations, the IoT users are deployed in an area of size 1 km  $\times$  1 km. We consider this scenario in an urban environment with  $\alpha = 9.61$  and  $\beta = 0.16$  at 2.1 GHz carrier frequency. Table III defines the simulation parameters. Note that we reach to all the results after a large number of independent runs.

TABLE II  
COMPUTATIONAL COMPLEXITY

Kind of Problem	Computational Complexity
3DP Subproblem of LoS scheme	$\max \{3J + 1, I + 1\}^3 \times (3J + 1)^{0.5} \log(\frac{1}{\tilde{\mu}})$
JRU Subproblem of LoS Scheme	$\frac{\log(\frac{4IMJL+I+L}{\tilde{t}\tilde{\mu}})}{\log(\tilde{\xi})}$
3DP Subproblem of Generalized Scheme	$\frac{\log(\frac{5IJ}{\tilde{t}\tilde{\mu}})}{\log(\tilde{\xi})}$
JRU Subproblem of Generalized Scheme	$\frac{\log(\frac{4IMJL+I+L}{\tilde{t}\tilde{\mu}})}{\log(\tilde{\xi})}$

TABLE III  
SIMULATION PARAMETERS

$f_c$	carrier frequency	2.1GHz
$\delta$	bit error rate	$10^{-8}$
$N_0$	noise power spectral density	-170 dBm
$\xi_{LoS}$	additional loss for LoS	1.6dB
$\xi_{NLoS}$	additional loss for NLoS	23dB
$n$	path loss exponent	2
$\alpha$	constant value for $P_{LoS}$	9.61
$\beta$	constant value for $P_{LoS}$	0.16

Fig. 2 indicates that which user is connected to which ABS and shows the efficient locations of ABSs should be deployed. In this figure, we have 5 ABSs to support 80 IoT users. Note that, each ABS can be allocated to at most 25 IoT users because of resource block limitation. Therefore, the maximum size of the IoT user clusters is 25. It is obvious that the location of IoT users affects on the number of users per cluster and also the efficient locations of the ABSs. Note that, the minimum and maximum IoT user cluster sizes are 10 and 20, respectively. Fig. 3 shows the 3-D view of ABSs deployment, and hence, we can see that ABSs altitude affects on the number of IoT users to support.

Fig. 4 shows the average ABS altitude versus the number of the ABSs for two different channel models which we use in our system model as LoS scheme and generalized scheme. Note that, by increasing the number of ABSs, the average ABS altitude decreases. By increasing the number of ABSs, overlapping between the coverage regions of the ABSs increases. Therefore, the coverage radius of ABSs must be decreased by reducing their height. More over, in the generalized scheme the ABSs can see the users in dense area as LoS and see other users as NLoS. Therefore, the average ABS altitude reduces in generalized scheme in comparison with the LoS scheme. Due to the fact that ABSs in higher altitude need more transmit power, and hence, the overall transmit power of IoT users in generalized scheme is lower than the overall transmit power in LoS scheme as shown in Fig. 5.

Fig. 5 shows the overall transmit power of IoT users versus the number of ABSs. In this figure, the performance of the proposed methods is compared with the fixed ABSs case which considers that the locations of ABSs are known. In the fixed ABSs case, assuming a uniform distribution of IoT users, we fix the location of ABSs at an altitude of 550 m, and then, we assign each IoT user to the nearest ABS. Therefore, in the fixed ABSs case we have only RRA optimization problem. In

the next step, we can see that the maximum size of each cluster decreases as the number of ABSs increases. Furthermore, we can see that the generalized scheme can be more efficient than the LoS scheme because the average altitude of ABSs decreases in the generalized scheme in comparison with the LoS method. Note that, the proposed generalized model does not spoil the LoS ability of ABSs. For example, consider a number of users that most of them are densified in an area but a few numbers are far from the majority. If we use the LoS scheme for deployment of ABSs, we must deploy them in high altitudes that they can see all the users with LoS. But we can waiver the minority and deploy the ABSs in a way that they can only see the majority of IoT users as LoS. Not only this assumption does not spoil the LoS ability of ABSs, but also it can make our method more efficient in practical cases. As expected, increasing the number of ABSs reduces the overall transmit power of IoT users.

Fig. 6 shows the overall transmit power of the IoT users versus the number of the ABSs. We can see, using two modulation order (QPSK+8PSK) is more efficient in comparison with (QPSK). Using different modulation orders makes the ABSs more flexible than before in order to choose the best option for connection, and hence, the Overall transmit power of the IoT users decreases in comparison with the case using one modulation order. As expected, the total transmit power of the generalized model is lower than the LoS method.

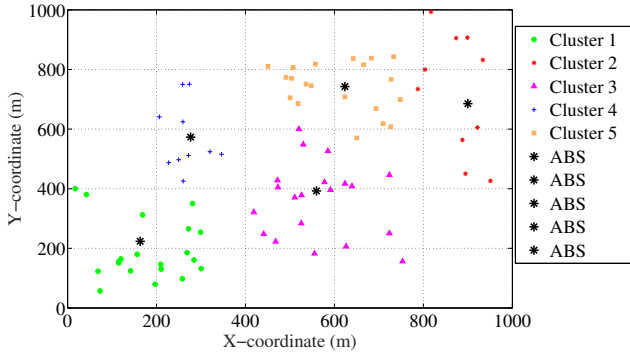


Fig. 2. User association and 2D placement of ABSs considering the case with only the LoS

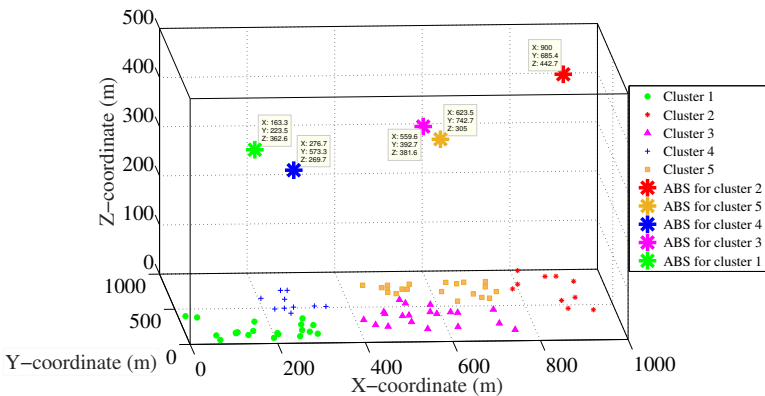


Fig. 3. User association and 3D placement of ABSs considering the case with only the LoS

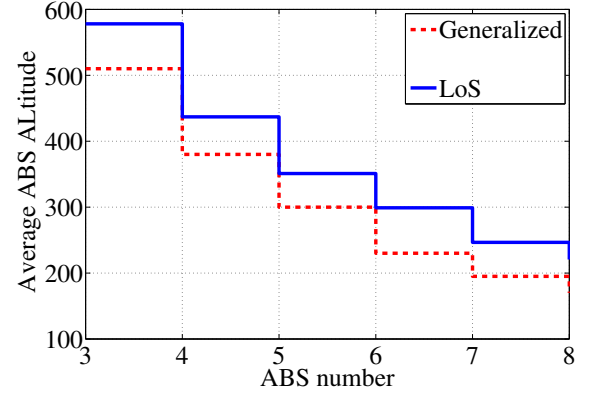


Fig. 4. The average ABS altitude vs. the number of the ABSs in two cases: LoS and generalized

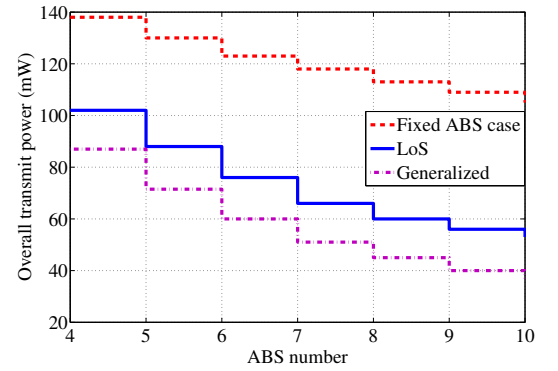


Fig. 5. The overall transmit power of IoT users vs. the number of the ABSs in three cases: fixed ABS case, LoS and generalized

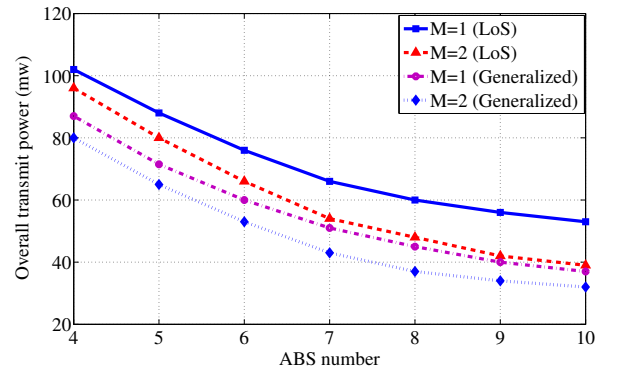


Fig. 6. The total transmit power of IoT users vs. the number of the ABSs in two schemes considering different modulation orders

## VI. CONCLUSION

In this paper, we investigated the joint RRA, 3DP, and user association for ABSs in IoT networks considering adaptive modulation. Note that, we considered two schemes with different channel models, namely, generalized scheme and LoS scheme. In our proposed methods, we found the efficient 3D locations of ABSs in order to minimize the overall transmit power of the IoT users satisfying some existing QoS Constraint. The results showed that by carefully clustering the IoT users and deploying the ABSs, the overall transmit power of the IoT users significantly decreases in comparison with



the fixed ABSs case. More over, the generalized scheme can be more efficient in some practical cases in comparison with the LoS scheme. As expected, by increasing the number of ABSs, overall transmit power of users decreases. Finally, we showed that by increasing the ABSs number, the average ABS altitude decreases, and hence, it is obvious that there is a trade off between number of ABSs and average ABS altitude. Note that, we use OFDMA technology for our proposed scenario. Accordingly, we want to study on some existing multiple access technologies in next generation such as sparse code multiple access (SCMA) and power domain non orthogonal multiple access (PD-NOMA) in order to use in our proposed scenario as future work. More over, we can extend our proposed system model into multi tier heterogeneous Base Stations which can make our model valid for next generation scenarios.

#### REFERENCES

- [1] M. Mozaffari, W. Saad, M. Bennis, and M. Debbah, "Unmanned aerial vehicle with underlaid device-to-device communications: Performance and tradeoffs," *IEEE Transactions on Wireless Communications*, vol. 15, no. 6, pp. 3949-3963, 2016.
- [2] I. Bekmezci, O. K. Sahingoz, and S. Temel, "Flying ad-hoc networks (FANETs): A survey," *Ad Hoc Networks*, vol. 11, no. 3, pp. 1254-1270, 2013.
- [3] D. Orfanus, E. P. de Freitas, and F. Eliassen, "Self-organization as a supporting paradigm for military UAV relay networks," *IEEE Communications Letters*, vol. 20, no. 4, pp. 804-807, 2016.
- [4] A. Hourani, S. Kandeepan, and A. Jamalipour, "Modeling air-to-ground path loss for low altitude platforms in urban environments," in *Proc. of Global Communications Conference (GLOBECOM)*, Austin, TX, USA, 8-12 Dec. 2014, pp. 2898-2904.
- [5] N. H. Motlagh, T. Taleb, and O. Arouk, "Low-altitude unmanned aerial vehicles-based internet of things services: Comprehensive survey and future perspectives," *IEEE Internet of Things Journal*, vol. 3, no. 6, pp. 899-922, 2016.
- [6] M. Razzaque, M. Milojevic, A. Palade and S. Clarke, "Middleware for internet of things: a survey," *IEEE Internet of Things Journal*, vol. 3, no. 1, pp. 70-95, 2016.
- [7] V. Angelakis, I. Avgouleas, N. Pappas, E. Fitzgerald and D. Yuan, "Allocation of heterogeneous resources of an IoT device to flexible services," *IEEE Internet of Things Journal*, vol. 3, no. 5, pp. 691-700, 2016.
- [8] A. Ngu, M. Gutierrez, V. Metsis, S. Nepal and Q. Sheng, "IoT middleware: A survey on issues and enabling technologies," *IEEE Internet of Things Journal*, vol. 4, no. 1, pp. 1-20, 2017.
- [9] C. Yin, Z. Xiao, X. Cao, X. Xi, P. Yang and D. Wu, "Offline and Online Search: UAV Multi-Objective Path Planning under Dynamic Urban Environment," *IEEE Internet of Things Journal*, 2017.
- [10] N. Motlagh, M. Bagaa and T. Taleb, "UAV-based iot platform: A crowd surveillance use case," *IEEE Communications Magazine*, vol. 55, no. 2, pp. 128-134, 2017.
- [11] Z. Dawy, W. Saad, A. Ghosh, J. G. Andrews, and E. Yaacoub, "Toward massive machine type cellular communications," *IEEE Wireless Communications*, vol. 24, no. 1, pp. 120-128, 2017.
- [12] S.Y. Lien, K.C. Chen, and Y. Lin, "Toward ubiquitous massive accesses in 3GPP machine-to-machine communications," *IEEE Communications Magazine*, vol. 49, no. 4, 2011.
- [13] H. S. Dhillon, H. Huang, and H. Viswanathan, "Wide-area wireless communication challenges for the Internet of Things," *IEEE Communications Magazine*, vol. 55, no. 2, pp. 168-174, 2017.
- [14] R. Yaliniz, A. El-Keyi, and H. Yanikomeroglu, "Efficient 3-D placement of an aerial base station in next generation cellular networks," in *Proc. of Communications (ICC)*, Kuala Lumpur, Malaysia, 22-27 May 2016, pp. 1-5.
- [15] A. Hourani, K. Sithampanathan, and S. Lardner, "Optimal LAP altitude for maximum coverage," *IEEE Wireless Communications Letters*, vol. 3, no. 6, pp. 569-572, 2014.
- [16] J. Kosmerl and A. Vilhar, "Base stations placement optimization in wireless networks for emergency communications," in *Proc. of Communications (ICC)*, Sydney, NSW, Australia, 10-14 June 2014, pp. 200-205.
- [17] A. M. Hayajneh et al, "Optimal Dimensioning and Performance Analysis of Drone-Based Wireless Communications," in *Proc. of Globecom Workshops (GC Wkshps)*, Washington, DC, USA, 4-8 Dec. 2016, pp. 1-6.
- [18] M. Alzenad, M. Z. Shakir, H. Yanikomeroglu, and M. Alouini, "FSO-based vertical backhaul/fronthaul framework for 5G+ wireless networks," *arXiv preprint arXiv:1607.01472*, 2016.
- [19] M. Mozaffari, W. Saad, M. Bennis, and M. Debbah, "Drone small cells in the clouds: Design, deployment and performance analysis," in *Proc. of Global Communications Conference (GLOBECOM)*, San Diego, CA, USA, 6-10 Dec. 2015, pp. 1-6.
- [20] M. Mozaffari, W. Saad, M. Bennis, and M. Debbah, "Efficient deployment of multiple unmanned aerial vehicles for optimal wireless coverage," *IEEE Communications Letters*, vol. 20, no. 8, pp. 1647-1650, 2016.
- [21] V. Sharma, R. Sabatini and S. Ramasamy, "UAVs assisted delay optimization in heterogeneous wireless networks," *IEEE Communications Letters*, vol. 20, no. 12, pp. 2526-2529, 2016.
- [22] V. Sharma, M. Bennis and R. Kumar, "UAV-assisted heterogeneous networks for capacity enhancement," *IEEE Communications Letters*, vol. 20, no. 6, pp. 1207-1210, 2016.
- [23] A. Merwaday, A. Tuncer, A. Kumbhar and I. Guvenc, "Improved throughput coverage in natural disasters: Unmanned aerial base stations for public-safety communications," *IEEE Vehicular Technology Magazine*, vol. 11, no. 4, pp. 53-60, 2016.
- [24] A. Merwaday and I. Guvenc, "UAV assisted heterogeneous networks for public safety communications," in *Proc. of Wireless Communications and Networking Conference Workshops (WCNCW)*, New Orleans, LA, USA, 9-12 March 2015, pp. 329-334.
- [25] Q. Wang, Z. Chen, W. Mei, J. Fang, "Improving physical layer security using UAV-enabled mobile relaying," *IEEE Wireless Communications Letters*, 2017.
- [26] M. Soorki, M. Mozaffari, W. Saad, M. Manshaei and H. Saidi, "Resource allocation for machine-to-machine communications with unmanned aerial vehicles," in *Proc. of Globecom Workshops (GC Wkshps)*, Washington, DC, USA, 4-8 Dec. 2016, pp. 1-6.
- [27] J. Li and Y. Han, "Optimal resource allocation for packet delay minimization in multi-layer UAV networks," *IEEE Communications Letters*, vol. 21, no. 3, pp. 580-583, 2017.
- [28] Z. Han, A. L. Swindlehurst, and K. Liu, "Optimization of MANET connectivity via smart deployment/movement of unmanned air vehicles," *IEEE Transactions on Vehicular Technology*, vol. 58, no. 7, pp. 3533-3546, 2009.
- [29] M. Mozaffari, W. Saad, M. Bennis, and M. Debbah, "Optimal transport theory for power-efficient deployment of unmanned aerial vehicles," in *Proc. of Communications (ICC)*, Kuala Lumpur, Malaysia, 22-27 May 2016, pp. 1-6.
- [30] A. Fotouhi, M. Ding, and M. Hassan, "Dynamic base station repositioning to improve performance of drone small cells," in *Proc. of Globecom Workshops (GC Wkshps)*, Washington, DC, USA, 4-8 Dec. 2016, pp. 1-6.
- [31] E. Kalantari, M. Z. Shakir, H. Yanikomeroglu, and A. Yongacoglu, "Backhaul-aware robust 3D drone placement in 5G+ wireless networks," *arXiv preprint arXiv:1702.08395*, 2017.
- [32] M. Mozaffari, W. Saad, M. Bennis, and M. Debbah, "Mobile Internet of Things: Can UAVs provide an energy-efficient mobile architecture?," in *Proc. of Global Communications Conference (GLOBECOM)*, Washington, DC, USA, 4-8 Dec. 2016, pp. 1-6.
- [33] M. Chen and M. Mozaffari, W. Saad, C. Yin, M. Debbah, C. Hong "Caching in the sky: Proactive deployment of cache-enabled unmanned aerial vehicles for optimized quality-of-experience," *IEEE Journal on Selected Areas in Communications*, vol. 35, no.5, pp. 1046-1061, 2017.
- [34] X. Li, D. Guo, and H. Yin, G. Wei "Drone-assisted public safety wireless broadband network," in *Proc. of Wireless Communications and Networking Conference Workshops (WCNCW)*, New Orleans, LA, USA, 9-12 March 2015, pp. 323-328.
- [35] P. Zhan, K. Yu and L. Swindlehurst "Wireless relay communications with unmanned aerial vehicles: Performance and optimization," *IEEE Transactions on Aerospace and Electronic Systems*, vol. 47, no.3, pp. 2068-2085, 2011.
- [36] A. Abdulla, Z. Fadlullah, H. Nishiyama, N. Kato, F. Ono, R. Miura "Toward fair maximization of energy efficiency in multiple UAS-aided networks: A game-theoretic methodology," *IEEE Transactions on Wireless Communications*, vol. 14, no. 1, pp. 305-316, 2015.
- [37] A. Goldsmith, *Wireless Communications*, Cambridge university press, 2005.
- [38] S. Boyd, S. Kim, L. Vandenberghe and A. Hassibi, "A tutorial on geometric programming," *Optimization and engineering*, Springer, vol. 8, no. 1, 2007.

- [39] S. Boyd and L. Vandenberghe, "A tutorial on geometric programming," *Cambridge university press*, 2004.
- [40] Z. Luo, W. Ma, A. So, Y. Ye and S. Zhang "Semidefinite relaxation of quadratic optimization problems," *IEEE Signal Processing Magazine*, vol. 27, no. 3, pp. 20-34, 2010.